EUROPEAN ORGANIZATION FOR NUCLEAR RESEARCH

ALICE-ANA-2017-xxx
March 5, 2018

Multiplicity dependent production of heavy-flavour decay electrons in p–Pb collisions at $\sqrt{s}$ = 8.16 TeV

P. Dhankher[1], D. Thomas[2], R. Varma[1]

1. Indian Institute of Technology, Bombay
2. The University of Texas, Austin

Email: preeti.dhankher@iitb.ac.in, deepa.thomas@cern.ch, raghava.varma@iitb.ac.in

Abstract

In this work, we will present the measurement of the self-normalised yield of electrons from heavy-flavour hadron decay as a function of the self-normalised charged-particle multiplicity in the transverse momentum range $3 < p_T < 35$ GeV/c in p-Pb collisions at $\sqrt{s_{\rm NN}}$ = 8.16 TeV with ALICE at the LHC. The charged-particle multiplicity is estimated using the SPDTracklets at mid–rapidity $|\eta| < 1$ and the V0 detector at forward rapidity.

Keywords: Heavy-flavour electrons, self-normalised yield, multiplicity, p-Pb collisions

Contents

1 Introduction

Heavy quarks (charm and beauty), produced in the initial stages of hadronic collisions in hard scattering processes, provide an important testing ground for perturbative QCD calculations. Measurements of their production as a function of the charged-particle multiplicity in pp and p-Pb collisions have recently gained interest for investigating the interplay between hard and soft mechanisms of particle production. In the p-Pb collision system, the formation and the kinematic properties of heavy-flavour hadrons can be influenced at all stages by Cold Nuclear Matter (CNM) effects and by concurrent Multiple Parton Interactions (MPI).

In recent studies, a faster than linear increase of the self-normalised yield of electrons from heavy-flavour hadrons as a function of charged-particle multiplicity up to 8 GeV/c has been observed in p-Pb collisions at $\sqrt{s_{\mathrm{NN}}}$ = 5.02 TeV. Such trend can arise from the interplay between MPI and multiple binary nucleon-nucleon collisions. To further explore the non linear rise, we extend these measurements to higher p_{T} where the contribution of electrons from beauty-hadron decays is expected to dominate.

2 Experimental Apparatus

The ALICE detector with an overall dimension of $16 \times 16 \times 26$ m^3 has high detector granularity, a low momentum threshold $p_T^{min} \approx 0.1$ GeV/c, and good particle identification capabilities up to 20 GeV/c. In this note, only detectors which are relevant for this analysis are briefly described whereas the detailed description of ALICE apparatus can be found in [52]. The ALICE apparatus is mainly divided into the central barrel and forward detectors. The central barrel, which is situated inside the large solenoid with a uniform magnetic field of 0.5 T parallel to the LHC beam line, covers the pseudorapidity region $|\eta| < 0.9$ and provides particle reconstruction and identification. The forward detectors contain a forward muon spectrometer with the pseudorapidity coverage of $-4 < \eta < -2.5$ and a set of small detectors used for trigger and event characterisations. The ALICE detector uses right-handed orthogonal Cartesian coordinate system with the origin at the geometrical centre of the central barrel, the z axis points towards LHC Beam 2 (anticlockwise) along the beam line, the x axis in the horizontal plane directed towards the centre of the LHC, and the y axis, consequently, points upward. The detector performance for measurements in LHC Run 1 with different collision systems is reported in [53].

The Inner Tracking System (ITS) is the innermost detector of the ALICE central barrel with six cylindrical layers of silicon detectors placed radially between 3.9 cm and 43.0 cm from the beam line, covering full azimuth. The main tasks of the ITS are to provide reconstruction of the primary vertex and secondary vertex which allows the separation of charm and beauty-hadron decay vertices, which boost the momentum and angle resolution for reconstructed particles provided by the TPC. The ITS provides tracking and identification of particles with very low p_{T}, which are unable to reach the TPC. It further supplements the TPC to provide reconstruction of particles transversing the dead regions of TPC [54]. The first two layers from the beam line are made up of Silicon Pixel Detectors (SPD) and placed at a radial distance of 3.9 cm and 7.6 cm from the beam line. The SPD contains overall 1200 readout chips for a total of 9.8×10^6 pixels of size $50(r\varphi) \times 425(z)$ μm^2, which provides intrinsic spatial resolution of $12(r\varphi) \times 100(z)$ μm^2. The third and fourth layers, at a radial distance of 15.0 and 23.9 cm, are equipped with Silicon Drift Detectors (SDD). The SDD provides position resolution better than 30 μm along z-direction and along the $r\varphi$, the position is determined from drift time with a resolution that depends on the calibration of the drift velocity. The two outermost layers, are located at a radii of 38.0 and 43.0 cm and are made up of Silicon Strip Detectors (SSD). The SSD consist of double-sided silicon strip sensor modules and provides intrinsic spatial resolution of $20(r\varphi) \times 830(z)$ μm^2. In pp collisions, the resolution of d_0 (track impact parameter) measured by ITS, which is defined as signed distance of closest approach between the track and primary vertex in $r\varphi$ plane is better than 75 μm for $p_{\mathrm{T}} > 1$ GeV/c and reaches up to 30 μm for $p_{\mathrm{T}} > 10$ GeV/c [1, 53]. The survey information, cosmic-ray tracks, and pp data were used for the alignment of ITS modules using the method described in [55]. The material budget of the ITS layers is very low including the support structure, the electrical interfaces and the cooling system, the total material budget is on average 7.66% of radiation length, X_0 for perpendicular tracks. This limits the influence of the Coulomb multiple scattering [54].

The Time Projection Chamber (TPC) is the main tracking detector in the central barrel region and together with the ITS, using the Kalman filter algorithm [56] provides charged-particle tracks reconstruction. The TPC is made up of a large cylindrical drift detector and covers the active volume from the radii 85 cm to 247 cm from beam line and 500 cm along the beam direction, with pseudorapidity range of $|\eta| < 0.9$ and full azimuthal acceptance [57]. The material budget of the TPC is around 3.5% to 5% of X_0 from central to $|\eta| = 0.9$ rapidity. The TPC provides track reconstruction with up to 159 three-dimensional space points per track and with a measurement of the specific ionisation energy loss, dE/dx with the resolution of about 5.5% for tracks that traverse the full volume of the detector [58]. The TPC provides good momentum resolution for tracks in wide p_{T} range (from as low as 0.1 GeV/c up to 100 GeV/c). Its position resolution is $800 - 1100(r\varphi) \times 1100 - 1250(z)$ μm^2. Global tracks used in the reconstruction of primary and secondary vertices are constructed from the prolongation of the TPC tracks into the hits in the ITS layers.

The V0 detectors are used mainly for minimum-bias trigger along with the SPD and for beam-induced background rejection [60]. The minimum-bias collisions require at least one hit in either of the V0 counters or in the SPD ($|\eta| < 2$), simultaneously with arrival of proton bunches from both the directions. It is made up of two arrays of scintillator counters (V0C and V0A, 32 counters each) placed in the forward region, V0C, at 90 cm and backward region, V0A, at 340 cm from detector centre and covers the pseudorapidity regions $-3.7 < \eta < -1.7$ (V0C) and $2.8 < \eta < 5.1$ (V0A).

3 Analysis Framework and Event Selection

The analysis has been performed on 2016 p-Pb collisions at $\sqrt{s}$ = 8.16 TeV collected with ALICE detector. The analysed data are the LHC16r and LHC16s. Based on the performance of EMCal, DCal TPC,ITS and V0, the good runs are selected from the Run Condition Table(RCT).

3.1 Data Samples

The LEGO trains with run numbers –, and – were used to extract the raw yield results presented in this analysis note. The list of runs used for the analysis, for each of the data taking periods (LHC16r, LHC16s) is the following:

LHC16r: *266318, 266317, 266316, 266208, 266197, 266196, 266187, 26574;*

LHC16s: *267110, 267081, 267077, 267072, 267070, 266998, 266997, 266994, 266993, 266944, 266886, 266885, 266883, 266882, 266437;*

3.2 Monte Carlo Samples

The Monte Carlo (MC) data sample used to compute non-heavy flavour decay electron reconstruction efficiency and tracking efficiency is production LHC17i5b simulated using the HIJING event generator [68] and transported using GEANT 3 [71]. This Monte Carlo sample

– is anchored to EMCal trigger, high threshold EG1, pPb (Pbp) at 8.16 TeV (LHC16r + LHC16s).
– has enhanced sample of π^0 and η mesons in order to increase the statistics of electrons from π^0, η and γ.

The run numbers used in this production are the following:

LHC17i5b: *265744, 266187, 266196, 266197, 266208, 266316, 266317, 266318, 266437, 266882, 266883, 266885, 266886, 266944, 266993, 266994, 266997, 266998, 267070, 267072, 267077, 267081, 267110;*

The analysis has been performed using `AliAnalysisTaskHFEMultiplicity`, `AddTaskHFEMultiplicity` task, with AliRoot version `v5-09-05-1` and AliPhysics version `vAN-20170516-1`.

3.3 Trigger System

The rate of collision is higher than the rate that the ALICE detector can collect and record. So, a trigger system is activated to select the interesting events that should be measured by the ALICE detectors from the other non-interesting events.
The minimum bias trigger ensures that the collision is happend. When it is satisfied than all the detectors takes the data. The minimum bias(MB) trigger used in this analysis is kINT7 which requires a concidence of signals in the V0A and V0C detectors.

The ALICE detector capabilities are extended using the EMCal trigger. The EMCal trigger is used to select events with high p_T particles based on the energy deposited in the EMCal. The EMCal has a Level 0 trigger, Level 1-gamma trigger and Level 1-jet trigger.

1. L-0 trigger: The trigger patch has predefined area of 4×4 adjacent towers, or 2×2 adjacent modules. The energy is summed over sliding window of this area within Trigger Region Unit (TRU) border limit shown in figure 1.
2. L-1 gamma trigger: This trigger is similar to L-0 trigger except there is no TRU border limit to sum the energy.
3. L-1 jet trigger: The energy is summed over a sliding window of n x n subregions and a subregion is defined as 8×8 towers.

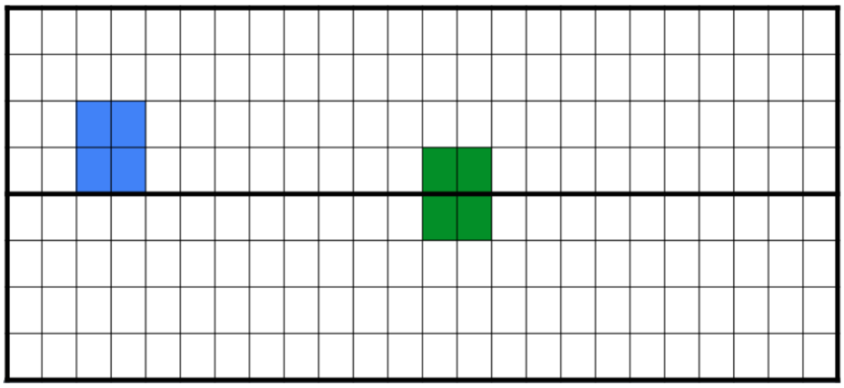

Fig. 1: Two EMCal TRU and examples of the L0 and L1 levels of trigger. L0 is shown in blue and only sum the energy inside a given TRU. L1 is shown in green and sum energy of two subsequents TRU.

In this analysis, we have L1-γ trigger for both EMCal(also called EG) and DCal(also called DG) and from the table 1, we can see EMCal and DCal have similar trigger conditions. So, we can combine them for the analysis.

Detector	Trigger Name	Level	Threshold(GeV)
EMCal	EG1	L1-γ	8
EMCal	EG2	L1-γ	5.5
DCal	DG1	L1-γ	8
DCal	DG2	L1-γ	5.5

Table 1: EMCal triggers for pPb events

3.4 Event Selection

The periods LHC16r and LHC16s have been merged for the analysis since they have similar trigger conditions. So, the run numbers used in this analysis contains minimum bias events, EMCal triggered events and DCal triggered events. The event cuts used to get good events for this selected sample are as follows:

1. Triggered events are selected with GA1 trigger fired ($E > 8$ GeV) and GA2 trigger fired ($E > 5.5$ GeV).
2. In all the three data samples, events are selected with a primary vertex position within 10 cm from the nominal center of the ALICE apparatus along the z-axis.

3. Events with both an SPD vertex and a primary vertex from tracks with at least one contributor.

4. The resolution of the z-position of the SPD vertex has to be smaller than 0.25 cm.

5. Pileup events are rejected by testing the event using the function IsPileupFromSPDInMultBins().

Figure 2 shows the total number of events, the number of analysed events along with the number of events rejected due to trigger selection, physics selection, primary vertex cuts, and pile-up rejection.

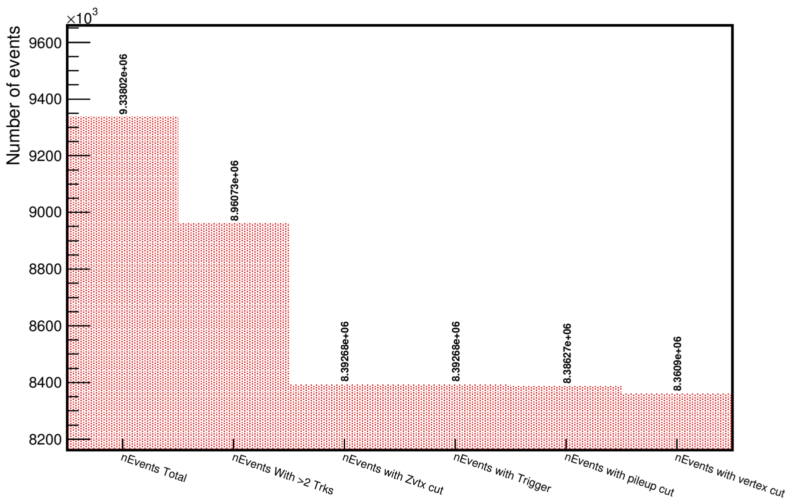

Fig. 2: Number of analysed.

3.5 EMCal correction framework

The EMCal different towers have different reponse to the same energy deposited. This is because of the presence of mis-alignment of modules and the bad channels which should be calibrated. The calibrations are based on the EMCal correction task, loaded in the runGrid macro as following:

```
AliTaskCDBconnect *taskCDB = AddTaskCDBconnect();
taskCDB->SetFallBackToRaw(kTRUE);

AliEmcalCorrectionTask * correctionTask = AddTaskEmcalCorrectionTask();
UInt_t kPhysSel = AliVEvent::kAny;
correctionTask->SelectCollisionCandidates(kPhysSel);

correctionTask->SetUserConfigurationFilename
("$ALICE_PHYSICS/PWGHF/hfe/macros/configs/pp/userConfigurationEMCele_pp_pPb.yaml");
correctionTask->Initialize();
```

Inside the task (.cxx) the tracks and cluster are loaded using the following:

```
fTracks_tender = dynamic_cast<TClonesArray*>(InputEvent()->FindListObject("tracks"));
fCaloClusters_tender =
dynamic_cast<TClonesArray*>(InputEvent()->FindListObject("caloClusters"));
```

The default configuration for pp and p-Pb analysis was used and can be found in:
`$ALICE_PHYSICS/PWGHF/hfe/macros/configs/pPb/userConfigurationEMCele_pp_pPb.yaml`.

4 Multiplicity Analysis

The production of heavy-flavour electron in p-Pb collisions has been studied as a function of charged-particle multiplicity estimated at mid-rapidity $|\eta| < 1$ and at forward rapidity.

4.1 Multiplicity Estimation

At mid-rapidity, the charged-particle multiplicity is estimated using SPDTracklets in $|\eta| < 1$. Tracklets are defined as the vectors spanned by combining the clusters in the SPD detector with the reconstructed primary vertex position. The mean number of Tracklets ($N_{\mathrm{tracklets}}$) has a linear dependence on the generated average charged primary particles. The proportinality factor is obtained by the monte carlo simulations of the detector response.
The event multiplicity at forward rapidity is estimated using the V0 scintillator. The aim of sudying the multiplicity dependence of heavy-flavour electron production also with this estimator is that the event multiplicity and the yields are evaluated in different pseudorapidity ranges and thus reducing the effects of auto-correlations.

4.1.1 SPD Tracklets Multiplicity

The raw number of SPD tracklets $N_{\mathrm{tracklets}}$ distribution can be seen in Figure for the two running periods “LHC16s” and “LHC16r”.

```
AliAODTracklets *tracklets = ((AliAODEvent*)ev)->GetTracklets();
nTracklets = tracklets->GetNumberOfTracklets();
for (Int_t nn = 0; nn < nTracklets; nn++)
Double_t theta = tracklets->GetTheta(nn);
Double_t eta = -TMath::Log(TMath::Tan(theta/2.0));
if (TMath::Abs(eta) < etaRange) nAcc++;
```

The left plot in figure 3 shows the mean number of tracklets along z_{vtx} position for LHC16s and LHC16r period of p–Pb run. It indicates that the distribution is not flat as a function of z_{vtx}. This is because of the inhomogenous acceptance of the SPD detector and variation in it as a function of time due to the varying number of active channels. So, a z-dependent data driven correction of the raw number ntracklets is applied to obtain a uniform distributed which we call $N^{\mathrm{corr}}_{\mathrm{tracklets}}$.

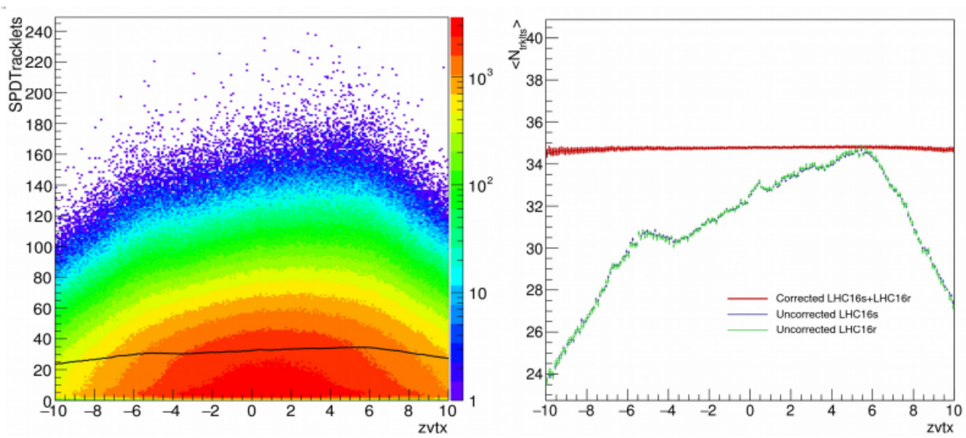

Fig. 3: Average of measured tracklets before (left: $N_{\mathrm{tracklets}}$) and after (right: $N^{\mathrm{corr}}_{\mathrm{tracklets}}$) corrections along $|z_{\mathrm{vtx}}| <$ 10 cm.

$$N_{\text{tracklets}}^{\text{corr}} = N_{\text{tracklets}} - Poisson\left(N_{\text{tracklets}} \cdot \left(\frac{< N_{\text{ref}} >}{< N_{\text{tracklets}} >} - 1\right)\right). \tag{1}$$

where, $\langle N_{\text{ref}} \rangle$ is reference value set to 34.8, which is the maxima of the plot of mean number of tracklets as a function of z_{vtx} bin. This reference value is same for period LHC16s and LHC16r as the $< N_{\text{tracklets}} >$ vs z_{vtx} distribution matches. Whereas, $\langle N_{\text{Tracklets}}(z) \rangle$ is an average number of tracklets for z_{vtx} positions for a particular period and $N_{\text{tracklets}}$ is a number of tracklets to be corrected in an event.
The right plot of figure 3 shows the distribution of corrected number of tracklets, $N_{\text{tracklets}}^{\text{corr}}$ both periods along z_{vtx} position compared to uncorrected distribution.

4.1.2 V0M Multiplicity

The production of heavy-flavour electron yield is also studied using V0 estimator. This estimator allows the measurement of multiplicity and HFE yield at two different pseudorapidity intervals (backward and central η), avoiding the possibilty of auto-correlations. The raw N_{V0M} frequency distribution can be seen in figure add reference here.

```
 AliAODVZERO *vzeroAOD =
dynamic_cast<AliAODVZERO *>(dynamic_cast<AliAODEvent *>(fAOD)->GetVZEROData());
Int_t V0AMult = static_cast<Int_t>(vzeroAOD->GetMTotV0A());
Int_t V0CMult = static_cast<Int_t>(vzeroAOD->GetMTotV0C());
Int_t V0Mult=V0AMult+V0CMult;
```

From the left plot in figure shows the mean V0M amplitude along z_{vtx} position for LHC16s and LHC16r period of p–Pb run. The average N_{V0M} also depends on z_{vtx} because of the variation in distance between the primary vertex and the detector array. This effect can be seen in the left plot of figure but it is less inhomogeneous than for the $< N_{\text{tracklets}} >[z_{vtx}]$ case. The distribution is corrected as follows:

```
Int_t vzeroMultACorr=V0AMult, vzeroMultCCorr=V0CMult, vzeroMultCorr=V0Mult;
vzeroMultACorr = static_cast<Int_t>(AliESDUtils::GetCorrV0A(V0AMult,Zvertex1));
vzeroMultCCorr = static_cast<Int_t>(AliESDUtils::GetCorrV0C(V0CMult,Zvertex1));
vzeroMultCorr = vzeroMultACorr + vzeroMultCCorr;
```

V0M corrected distribution can be seen in the right plot of figure.

4.2 Event multiplicity normalisation

4.2.1 Conversion from $N_{\text{tracklets}}$ to $\mathrm{d}N_{\text{ch}}/\mathrm{d}\eta$

Monte carlo information is used to convert from $N_{\text{tracklets}}^{\text{corr}}$ to “physical primaries” (N_{ch}). Physical primaries are the prompt particles and their decay products from the collision not considering those from the weak decay of strong particles. The proportionality factor between $N_{\text{tracklets}}^{\text{corr}}$ and N_{ch} is obtained by a linear fit to their 2D distribution show in figure 4. This factor is then applied to $N_{\text{tracklets}}^{\text{corr}}$ in each interval to get the estimated N_{ch} values.

The charged-particle pseudorapidity density($\mathrm{d}N_{\text{ch}}/\mathrm{d}\eta$) is evaluated by dividing the estimated N_{ch} values by considered η range($\Delta\eta$ = 2).

The uncertainity in estimating N_{ch} from $N_{\text{tracklets}}$ is evaluated by estimating its deviation from linearity. The linear fit is performed in different multiplicity bins and the proportionality factor obtained from the fit is compared with the multiplicity integrated resulting in 5%. This is shown in figure 4.

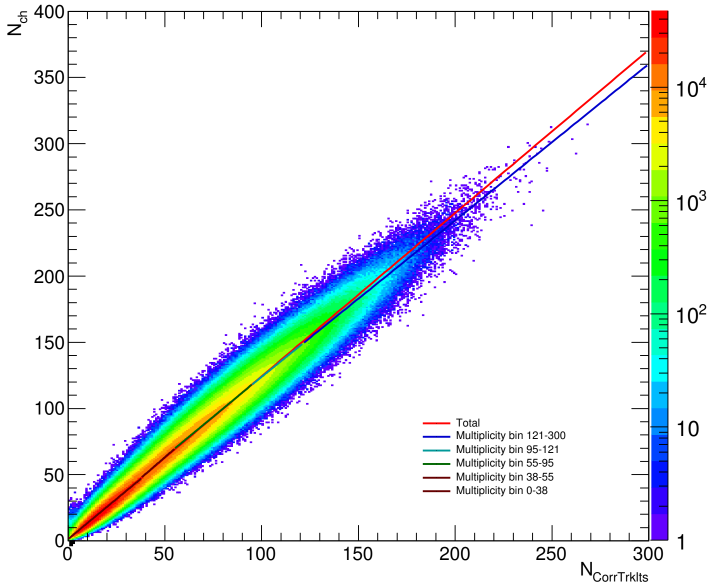

Fig. 4: N_{ch} as function of $N^{\mathrm{corr}}_{\mathrm{tracklets}}$ with linear fit to the total distribution and in different multiplicity intervals

Table 2: Multiplicity classes using $N_{\mathrm{tracklets}}$ as estimator and corresponding values for $\mathrm{d}N_{\mathrm{ch}}/\mathrm{d}\eta$.

$N_{\mathrm{tracklets}}$	$< N_{\mathrm{tracklets}} >$	α_i	$\mathrm{d}N_{\mathrm{ch}}/\mathrm{d}\eta / < \mathrm{d}N_{\mathrm{ch}}/\mathrm{d}\eta >$	relative error %	$N_{events}(\times 10^6)$
Integrated	34.7		-	-	
0-38				-	
38-55				-	
55-95				-	
95-121				-	
121-300				-	

4.2.2 V0M Multiplicity Normalisation

The average normalised event V0M multiplicity is obtained by normalising average V0M signal in a multiplicity interval by global average V0M signal. The different multiplicity bins and their corresponding number of events can be found in table.

Table 3: Multiplicity classes using N_{V0M} as estimator and corresponding values for $N_{V0M} / < N_{V0M} >$.

N_{V0M}	$< N_{V0M} >$	$\mathrm{N}_{V0M} / < N_{V0M} >$	$N_{events}(\times 10^6)$
Integrated		-	
0-38		-	
38-55		-	
55-95		-	
95-121		-	
121-300		-	

4.3 Trigger normalisation studies

The triggered events have been used in this analysis to increase the statistics of electrons at high p_T compared to minimum bias events. So, a normalising factor (S) is required to correct the triggered events to make them equivalent to minimum bias events. This can be extracted by dividing the cluster energy spectrum for each trigger with the minimum bias spectrum.

The trigger rejection is not multiplicity dependent and the multiplicity distribution is same whether we select the event from the MB or the triggered sample. This can be seen in figure. Since, we have to measure the per-event normalized yield, and the event normalization differs in MB and EG triggers, we need to use the relation of number of events in MB and EG to finally obtain the trigger normalisation factor (R) which is called trigger rejection factor. This is taken into account by the following equation:

$$S_{i,ev} = \frac{N_{ev,trig,i}}{N_{ev,MB,i}}.S \tag{2}$$

Where S (ratio of cluster energy distribution of trigger to cluster energy distribution of the minimum bias) is constant for all multiplicity bins,
$N_{ev,trig,i}$ ($N_{ev,MB,i}$) is the number of events in trigger (MB) data for the multiplicity bin i.
This S is related to the trigger rejection factor by the equation as follows:

$$S = \frac{1}{R} \tag{3}$$

5 Heavy-Flavour Electron Identification

The main aim of the analysis is to find the production cross-section and the multiplicity dependence of electrons at high p_T ($3 < p_T < 35$ GeV/c) from heavy-flavour hadron decays using the TPC+EMCal PID information. After the event selection, the next step is to select good tracks which successfully passes the quality cuts.

5.1 Track selection

The track cuts applied to select good tracks are listed in the below table. These cuts are optimized to have a high electron purity and low hadron contamination. The track in the TPC is reconstructed by combining the correlated clusters formed by particle traversing through the TPC medium. The maximum number of clusters in TPC is 159. So, a good electron candidate track require 100 clusters out of 159 for the reconstruction and in addition 80 clusters from these required number of cluster should have processable information for PID. To remove the contribution from the uncorrelated cluster to reconstructed track, a χ^2/NDF fit is performed for each cluster and it has to be smaller than 4.

To distinguish the track coming from the displaced weak decays and material interaction, a Distance of Clostest Approach (DCA) cut is imposed. A final refit of the track is done for ITS and TPC to remove the fake tracks and propagated to the EMCal detector using the kalman filter.

Table 4: Track selection cuts for electron identification.

Observable	Cut value
AOD filter bit required	kTrkGlobalNoDCA
TPC and ITS refit	required
χ^2/TPC cluster	< 4
Kink daughters	rejected
Number of ITS clusters	≥ 3
Number of TPC clusters	≥ 100
Number of TPC dE/dx clusters (PID clusters)	≥ 80
DCA to the primary vertex in radial direction	< 2.4
DCA to the primary vertex in z-direction	< 3.2

5.2 Electron Identification

Electrons can be identified using different detectors in ALICE in different momentum range. As this analysis is done at high p_T, the TPC and EMCal detectors are used for the PID. The particles in TPC are identified by using the information of the ionization energy loss(dE/dx) in the TPC. The dE/dx information is in the number of Nσ

5.3 Non-HFE reconstruction

5.3.1 Non-HFE reconstruction efficiency

6 Heavy-Flavour Electron vs Multiplicity

The multiplicity dependent analysis of electron from heavy-flavour hadron decays is done by measuring the self-normalised yield in different multiplicity bins. The self-normalised heavy-flavour electron yield is given by Eq 4.

$$HFE^{i}_{norm} = \frac{< HFE >^{i} /RF^{i} * N^{i}_{events}}{< HFE >^{0} /RF^{0} * N^{0}_{events}} \tag{4}$$

Where index ”i” denotes different multiplicity bins and the index ”0” represents the integrated mutiplicity. RF is the rejection factor. The analysis steps for this study is similar to the multiplicity independent analysis except we need to check the multiplicity dependence of the efficiencies. So, in the next section we show the results of the efficiencies as a function of multiplicity.

6.1 Efficiencies as a function of multiplicity

Tracking Efficiency

Photonic Tagging Efficiency

6.2 Self-Normalised Yield HFE

HFE self-normalised yield for SPDTracklets

Multiplicity bin	RF(GA1)	RF(GA2)
Integrated	780.351	250.893
1	1497.73	485.93
2	528.68	172.57
3	377.47	121.51
4	280.05	85.39
5	162.56	60.90

Table 5: Table for Trigger normalization factor

Table 6: Number of events and normalised HFE yield in multiplicity bins (MB) for $3 < p_T < 6$ GeV/c

Mult. bin	N_{events}	<HFE>	$\sigma_{<HFE>}$	HFE_{norm}	$\sigma_{<HFE_{norm}>}$	error/yield
Integrated						
1						
2						
3						
4						
5						

HFE self-normalised yield for V0M

Multiplicity bin	RF(GA1)	RF(GA2)
Integrated		
1		
2		
3		
4		
5		

Table 7: Table for Trigger normalization factor

Table 8: Number of events and normalised HFE yield in multiplicity bins (MB) for $3 < p_T < 6$ GeV/c

Mult. bin	N_{events}	<HFE>	$\sigma_{<HFE>}$	HFE_{norm}	$\sigma_{<HFE_{norm}>}$	error/yield
Integrated						
1						
2						
3						
4						
5						

7 Systematics Studies

In this section, we explore the possible systematic uncertainties

Observable	Reference	Min. Variation	Max. Variation
DCA_{xy} and DCA_z	2.4, 3.2	?	?
kink mother	rejected	accepted	–
ITS layer	3	2,4	6
TPC PID cluster	80	70, 90	110
TPC crossed rows cluster	100	90,110	80,120
TPC nsigma cut	(-1,3)	(-1.5,3.5)	(-0.5,2.5)
EMCAL PID(shower shape M20)	(0.02,0.35)	(0.015,0.4)	(0.025,0.3)
EMCAL PID E/P	(0.8,1.2)	(0.75,1.2)	(0.9,1.2)

Table 9: Table for systematic criteria for the inclusive electron

Observable	Reference	Min. Variation	Max. Variation
DCA_{xy} and DCA_z	2.4, 3.2	?	?
ITS layer	3	2,4	6
TPC cluster	80	70, 90	110
ITS refit	with refit	with no refit	
TPC nsigma cut	(-3,3)	?	?
Invariant mass cut	100	90	110

Table 10: Table for systematic criteria for the associated electron

7.1 Cut Variation Systematics

7.2 Systematic uncertainties in multiplicity sub-intervals

7.3 Summary of Systematics

track reconstruction efficiency expected to cancel out in the ratio of relative yields. The final systematic uncertainty assigned are summarised in the table 12.

Table 11: Summary of systematic uncertainties with estimator SPDTracklets.

p_{T} intervals (GeV/c)	$N_{\mathrm{tracklets}}$				
	0-38	38-55	55-95	95-121	121-300
3 - 6	-%	-%	-%	-%	-%
6 - 9	-%	-%	-%	-%	-%
9 - 12	-%	-%	-%	-%	-%
12 - 35	-%	-%	-%	-%	-%

Table 12: Summary of systematic uncertainties with estimator V0M.

p_T intervals (GeV/c)	$N_{\text{tracklets}}$				
	0-442	442-604	604-1014	1014-1273	1273-2000
3 - 6	-%	-%	-%	-%	-%
6 - 9	-%	-%	-%	-%	-%
9 - 12	-%	-%	-%	-%	-%
12 - 35	-%	-%	-%	-%	-%

8 Results and Summary